ADVANCED MATERIALS INTERFACES
www.advmatinterfaces.de

Tunable Drop Splashing on Magnetoactive Elastomers

*Gaia Kravanja, Inna A. Belyaeva, Luka Hribar, Irena Drevenšek-Olenik, Matija Jezeršek, and Mikhail Shamonin**

The significant effect of an external dc magnetic field on the splashing behavior of ethanol drops impacting on the unstructured (flat) surface of soft magnetoactive elastomers (MAEs) is reported. The Weber number corresponding to the transition between the deposition and the splashing regime is reduced by ≈20% in a moderate magnetic field of ≈300 mT. Alongside this effect, a two-fold increase of the initial deceleration of the ejection sheet is observed for the softest sample. The main underlying mechanism for the observed phenomena is believed to be the magnetic-field-induced stiffening of the MAEs. Further possible mechanisms are magnetically induced changes in the surface roughness and magnetic-field-induced plasticity (magnetic shape memory effect). The potential application areas are magnetically regulable wetting and magneto-responsive surfaces for controlling the drop splashing.

1. Introduction

Manipulation of drop splashing represents an important research area concerning the interaction between fluids and solids.[1,2] When a liquid drop impacts onto a solid surface, the drop may flatten and spread smoothly, or it may produce a ragged-edged splash. Both phenomena are crucial in various real-world applications. For instance, splashing should be suppressed in inkjet printing,[3] coating deposition,[4] nuclear safety engineering,[5] and prevention of disease transmission caused by aerosolization of contaminated liquids.[6] On the other hand, splashing is desirable in fuel combustion,[7,8] spray cooling,[9] or fire suppression.[10]

The outcome of the collision is determined by a number of factors, such as the surface topography and the rigidity of the bulk and subsurface material. For example, it has been recently shown that soft polymer coatings may offer a novel technical solution that can significantly reduce or even eliminate splashing.[11] However, hitherto it is not possible to change the mechanical properties of such coatings in a dynamically tunable way.

Magnetoactive elastomers (MAEs), also known as magnetorheological elastomers, are smart materials whose physical properties can be controlled by an external magnetic field.[2,12–20] They are hybrid materials[21] composed of a soft polymer matrix (organic constituent) with embedded ferromagnetic micrometer-sized particles (inorganic constituent). The majority of previous research concentrated on the bulk properties of MAEs. As far as bulk mechanical properties are concerned, MAEs become stiffer in higher magnetic fields. This means that their elastic moduli increase with an increasing magnetic field.[22] However, recently it has been realized that surface properties of MAEs are significantly modified in a magnetic field too. In particular, the wettability,[23–27] the surface roughness,[28–33] the adhesive properties,[23,24,34] and the friction phenomena[35–37] were all found to be strongly dependent on a magnetic field.

It is also well known that the magnetic field affects impact dynamics of ferrofluid drops onto rigid non-magnetic substrates,[38–40] but the case of a non-magnetic liquid drop impacting a magnetic substrate seems to be a hitherto neglected aspect of research.

The physical reason for the variation of both bulk and surface properties of MAEs is attributed to the restructuring of the magnetized filler particles, that is, changes in their mutual arrangement due to magnetic interactions between them. Significant reconfigurations in the microstructure can occur only in sufficiently soft polymer matrices. Therefore, attaining an appropriate matrix softness is one of the vital challenges related to MAE fabrication. In accordance with large magnetic-field-induced structural modifications of soft MAEs, it can be hypothesized that drop splashing on MAE surfaces will be affected by a magnetic field as well.

The purpose of this paper is to demonstrate the feasibility of tuning the splashing behavior of liquid drops on MAE surfaces by an external magnetic field. Based on the high-speed video-image analysis, we show that by changing the magnetic flux density, it is possible to switch between the impact regimes

G. Kravanja, L. Hribar, Prof. M. Jezeršek
Faculty of Mechanical Engineering
University of Ljubljana
Aškerčeva 6, Ljubljana SI-1000, Slovenia
I. A. Belyaeva, Prof. M. Shamonin
East Bavarian Centre for Intelligent Materials (EBACIM)
Ostbayerische Technische Hochschule (OTH) Regensburg
Seybothstr. 2, 93053 Regensburg, Germany
E-mail: mikhail.chamonine@oth-regensburg.de
Prof. I. Drevenšek-Olenik
Faculty of Mathematics and Physics
University of Ljubljana
Jadranska 19, Ljubljana SI-1000, Slovenia
Prof. I. Drevenšek-Olenik
Department of Complex Matter
J. Stefan Institute
Jamova 39, Ljubljana SI-1000, Slovenia
The ORCID identification number(s) for the author(s) of this article can be found under https://doi.org/10.1002/admi.202100235.

DOI: 10.1002/admi.202100235

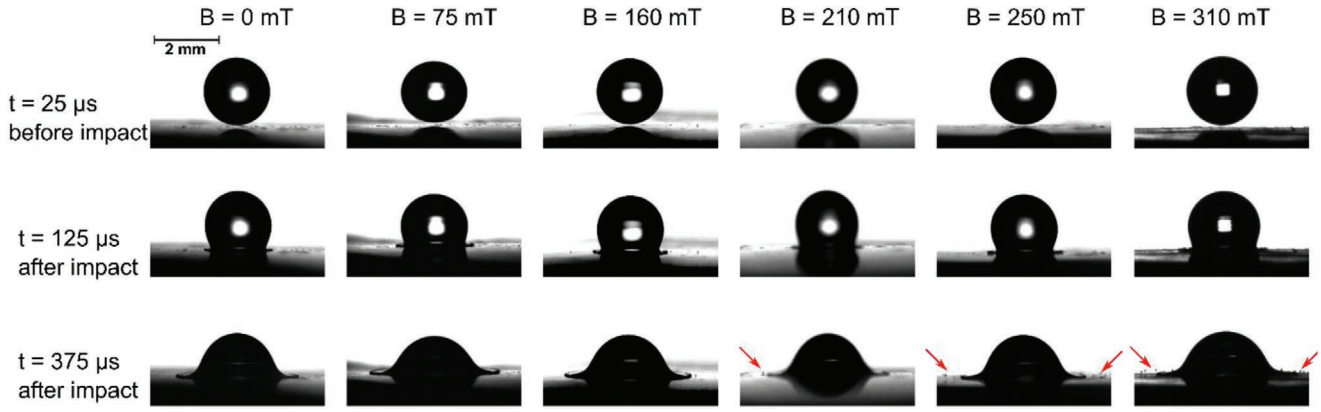

Figure 1. Video-sequences of drop impacts on the surface of a "soft" MAE (G_0' = 9 kPa) exposed to a vertical magnetic field of different flux densities B. The impact velocity in all cases corresponds to We = 191 ± 3.

of "deposition" and "splash." MAEs with three different values of shear storage moduli in the range of kPa are used as substrates. For all of them, the same effect is observed, namely an increasing inclination to splashing by increasing magnetic field.

2. Results

Drops of ethanol (≈5 μl) are controllably released from the needle positioned at some selected height above the MAE surface. **Figure 1** shows a set of typical images of drop splashes observed on the surface of a mechanically soft MAE exposed to a variable magnetic field. The field is oriented in the vertical direction perpendicularly to the MAE surface. The drop radius is R = 1.07 ± 0.012 mm and its impact speed is v = 2.24 ± 0.011 m s^{-1}. From these data, a dimensionless Weber number We = $\rho v^2 R/\sigma$ = 191 ± 3 is calculated, where σ = 0.0219 N m^{-1} is the surface tension and ρ = 789 kg m^{-3} the density of ethanol at room temperature. The Weber number corresponds to the ratio between the drop kinetic energy and its surface energy associated with surface tension. It is a parameter customary used in modeling microfluidics and multiphase flows that are two typical phenomena taking place during drop impacts.[41] The described experimental conditions correspond to those used in the work of Howland et al.[11] The conditions are such that the substrate wettability should not affect the impact behavior. Red arrows point toward several small droplets that are ejected from the ejection sheet at magnetic fields B > 160 mT. For B < 160 mT, no such droplets are generated. So, at B = 160 mT the transition from the deposition to the splashing regime takes place.

Figure 2a shows the values of We at which the transition from deposition to splashing occurs as a function of B for all three investigated MAE samples. Solid lines represent the boundary values corresponding to 50% probability of splashing, and confidence intervals correspond to 15–85% probability of splashing.

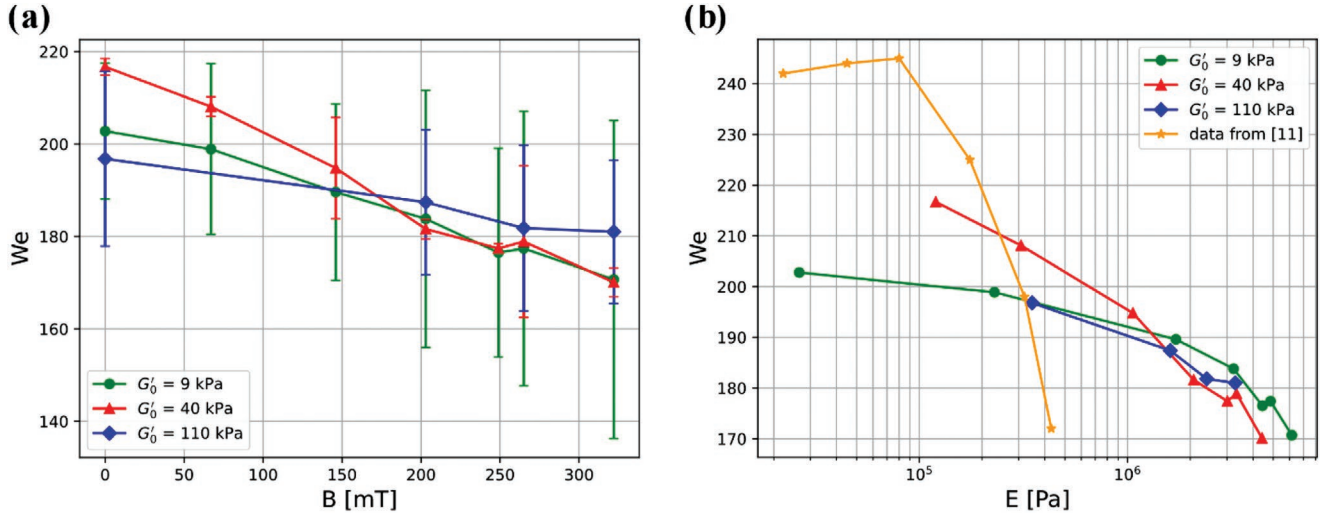

Figure 2. a) Weber number corresponding to the transition between the deposition and the splashing regime as a function of a magnetic field applied to the MAE. Solid lines correspond to 50% probability for splashing and confidence intervals depict splashing probability between 15% and 85%. Results obtained for three different MAE compositions are shown: "soft" (green circles), "medium" (red triangles), and "hard" (blue diamonds). b) Weber number corresponding to 50% probability for splashing as a function of the Young modulus of the substrate. Green circles, red triangles, and blue diamonds correspond to the measurements performed with MAE samples, while yellow stars are data for different silicones taken from ref. [11].

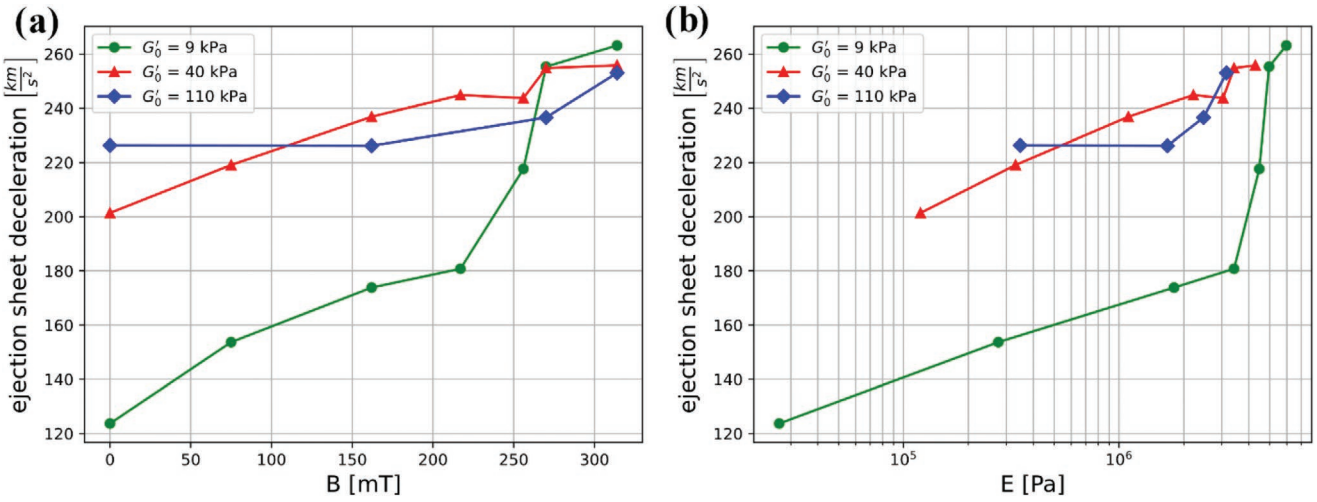

Figure 3. a) Initial deceleration of the ejection sheet as a function of B. b) Initial deceleration of the ejection sheet as a function of E. The results are obtained at We = 191 ± 3 and t = 25 µs.

Figure 2b shows the same values of We at which transition from deposition to splashing occurs, but this time plotted versus the Young's modulus E of the MAE substrates. The values of the latter were calculated from the data on shear storage modulus as a function of B (described in the Experimental Section) by assuming that MAEs are incompressible neo–Hookean solids, for which $E = 3G$,[42] and taking the low-frequency shear storage modulus G' as a reasonable approximation for static G. Here, only the lines corresponding to 50% probability of splashing are shown for clarity. For comparison, the yellow curve shows the data from the study reported in,[11] where pure silicone materials with different Young's moduli were used. The Young's moduli in[11] were measured by static indentation. All other experimental conditions in[11] were similar to ours.

Figure 3a shows an initial deceleration of the ejection sheet as a function of B measured at We = 191 ± 3 and t = 25 µs, which is obtained using the measurements of the ejection sheet radius shown in Figures S1–S3, Supporting Information, the procedure is described in the Supporting Information. For all three MAE materials, the magnitude of deceleration increases with increasing magnetic field.

Figure 3b shows the initial deceleration of the ejection sheet shown in Figure 3a against Young's moduli of the MAE materials at We = 191 ± 3 and t = 25 µs. For all three MAE materials, the magnitude of deceleration increases with increasing Young's modulus.

Figure 4a shows the dynamic contact angle of the ejection sheet measured during the drop impact events corresponding to We = 130 ± 7. Empty circles represent values obtained in the absence of a magnetic field, while full circles correspond to the values obtained at B = 250 mT. The data are plotted as a function of the ejection sheet velocity. The deposition starts with

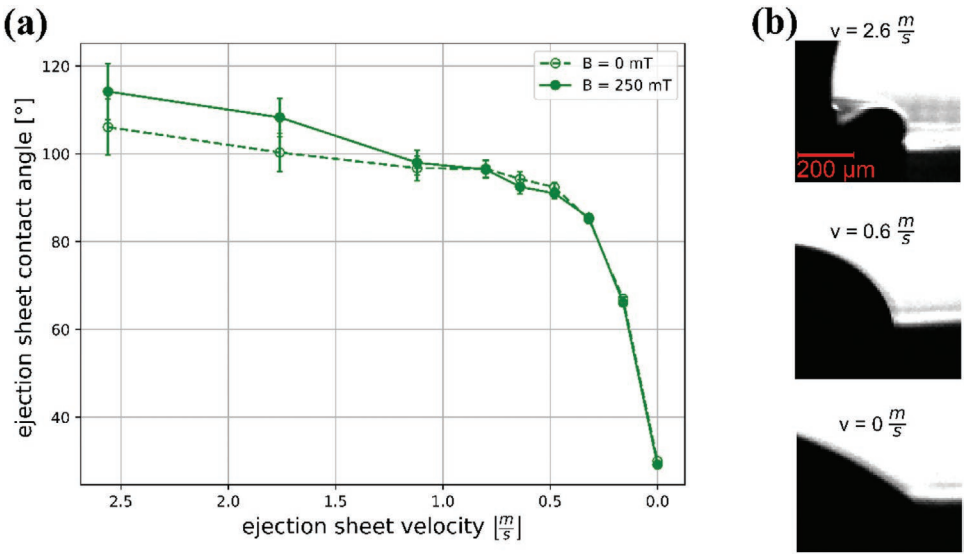

Figure 4. a) Ejection sheet contact angle as a function of ejection sheet velocity. b) Images of the ejection sheet tip at different velocities. The results are obtained at We = 130 ± 7.

the highest ejection sheet velocity of around 2.5 m s^{-1}, at which contact angles of around 105° and 115° are observed for $B = 0$ and $B = 250$ mT, respectively. Then the velocity decreases down toward zero when the rim stops. The values of contact angle at this point are around 30° for both $B = 0$ and $B = 250$ mT. The images of the ejection sheet tip at different velocities are shown in Figure 4b. The results shown in Figure 4 are similar to the results of Quetzeri-Santiago et al.,[43] who examined the dynamic contact angle of ethanol drops on glass surfaces.

3. Discussion

The possibility for manipulation of drop splashing on MAE surface with changing the magnetic flux density B is clearly demonstrated in Figure 1 and Figure 2a. At the drop velocity corresponding to We = 191 ± 3, it can be observed that at $B = 0$ mT, a deposition regime is detected for all three MAE compositions, while at $B = 250$ mT, splashing occurs for all of them. Resilience, which is defined as the ability of the material to absorb energy when it is elastically deformed, can explain why the splashing threshold decreases with increasing magnetic flux density. By increasing the magnetic flux density, Young's modulus of MAE increases, while the drop impact energy remains the same. Consequently, less kinetic energy is absorbed by the substrate. This effect is reflected in the initial deceleration of the ejection sheet, which increases with the increasing magnetic field density, as can be observed in Figure 3a. Larger deceleration causes larger inertial forces that break the rim into droplets.[11]

At the very early stage of the ejection sheet movement, in which motion is so fast, it is reasonable to assume that the viscoelastic solid behaves initially as an elastic substrate and inertial forces dominate ejection sheet dynamics, similar to the early drop spreading.[44,45] The time dependencies of the ejection sheet radius were found to fit to the power law $R_S \sim Ct^{\alpha}$ and the exponent α was in the range from 0.34 to 0.69, being in a reasonable agreement with the typical range from 0.25 to 0.5 for early drop spreading[44] (cf. Figures S1–S3 and Tables S1–S3, Supporting Information). However, it is known that impact of water droplets on soft viscoelastic surfaces exhibits complex phenomena and dynamics,[45] therefore the effect of viscoelasticty of MAE on drop splashing has to be investigated in more detail in future works.

Note that the loss tangent (the damping factor), which is the ratio of the loss modulus to the storage modulus ($\tan\delta = G''/G'$) decreases with the increasing magnetic field for all three samples. Therefore, the presented MAE materials become not only stiffer in magnetic fields, but also "more elastic," that is, the relative viscous contribution diminishes.

Similar effect of a magnetic field on deposition/splashing transition of water drops can be expected. However, for the same We, one would need to realize higher velocity of a water drop, because of the larger surface tension in comparison with ethanol.

The observed threshold values of We for 50% probability of splashing on the investigated MAE samples (Figure 2b) are somewhat lower than those reported for pure silicone materials in.[11] However, in both cases, the increased tendency for splashing with the increasing Young's modulus is evident. The differences between the silicones in[11] and the MAEs are attributed to possible differences in the chemical composition of the elastomer matrix and the presence of a ferromagnetic filler. Commercial silicone formulations may contain hidden components which are intentionally kept unknown as a secret recipe.[46] Furthermore, the elastic moduli obtained by dissimilar methods (e.g., static indentation and rheological measurements) may be somewhat different. The observed slope $\Delta We/\Delta E$ for MAE samples is also lower than for silicones. This discrepancy might be related to differences between the bulk and the surface elastic properties of MAEs. As reported in our recent paper, under the top surface of MAEs, there exists a thin (≈20 μm) depletion layer with a reduced concentration of magnetic microparticles.[28] The effect of magnetic field on elastic properties of this depletion layer can be different from its effect on the bulk medium.

An additional phenomenon that can influence the splashing behavior on MAE surface is magnetic-field-induced surface topographical changes. Optical microscopy images of the surface topography have been presented in refs. [25,26,28] and the surface roughness has been measured in refs. [26,28]. Recent investigations have shown that the surface roughness of isotropic MAEs increased with increasing magnetic field density (the responsivity was ≈1 μm T^{-1}), which consequently affected the wetting characteristics of the material.[26] In the present work, this effect can be seen in Figure 4, where during the initial stages of ejection sheet spreading (v >1.5 m s^{-1}), one can notice significant differences between the dynamic contact angles measured at $B = 0$ and at $B = 250$ mT. Since most of the droplets are ejected at this initial stage, their larger contact angle in the magnetic field promotes the splashing.

Despite the fact that some of the above-described phenomena are already relatively well known, further investigations are needed before a clear picture of their importance for drop splashing on MAE surface can be obtained. To avoid any repercussion of the ethanol deposition on surface properties of an MAE,[47–50] the samples were moved a little bit after each impact, so that a new drop always hit a virgin part of the surface. An observed after-effect is described in the Supporting Information. The details of the interaction between the ethanol and the MAE surface should be addressed in future work.

4. Conclusion

In summary, our work provides the proof of principle for the control of drop splashing on the surface of soft MAEs with an applied external magnetic field. It also provides an explanation of the main underlying mechanism of this effect, which is believed to be the magnetic-field-induced stiffening of the MAE. But, very probably also various additional phenomena, like modifications of surface roughness and plastic deformation of the surface, come into play. To find out the origin of those phenomena and their importance in splashing dynamics, further systematic measurements with different MAE compositions and different types of liquids need to be performed.

5. Experimental Section

This section describes the MAE sample preparation, the experimental setup for modifying the magnetic field and monitoring of drop splashing, and the measurement procedures for splash detection and subsequent analysis of the temporal variation of dynamic contact angle and diameter of the advancing ejection sheet.

MAE Sample Preparation: The samples were synthesized in the form of an MAE film coating on a transparent polyvinyl chloride (PVC) foil with a diameter of 33 mm and a total thickness of ≈2 mm. All three investigated compositions contained the same content of soft-magnetic carbonyl iron powder (CIP, type SQ, BASF SE Carbonyl Iron Powder & Metal Systems, Ludwigshafen, Germany) of 80 wt% (≈33 vol%). The CIP particles, which are known to have practically a spherical shape, had a mean (d50) diameter of 3.9–5.0 µm and no surface coating. The samples differed in their effective shear storage modulus in the absence of a magnetic field of ≈9, 40, and 110 kPa. These samples were denoted as "soft," "medium," and "hard," respectively.

The synthesis of the MAE materials followed the known path.[51,52] The samples were synthesized in several stages. For the initial compound, the polymer VS 100 000 (vinyl-functional polydimethylsiloxane), the polymer MV 2000 (monovinyl functional polydimethylsiloxane), the modifier 715 (SiH-terminated polydimethylsiloxane) from Evonik Hanse GmbH (Geesthacht, Germany) were put together and mixed with the silicone oil AK 10 (linear, nonreactive polydimethylsiloxane) from Wacker Chemie AG, Burghausen, Germany. In the next step, the initial compound was mixed with CIP SQ and then with the cross-linker 210 (dimethyl siloxane-methyl hydrogen siloxane copolymer). In the authors' case, the variation of the shear modulus in the absence of a field was achieved by changing the ratio of the molar concentrations of vinyl and hydride groups in the initial compound by adding different doses of the hydride-group containing component (crosslinker 210).[46,53] An increase in the stoichiometry, which was the ratio of the molar concentrations of hydride and vinyl reactive groups, leads to a stiffer polymer matrix, when the stoichiometry remains less than approximate unity. The cross-linking reaction was activated by the Pt-Catalyst 510 (0.067 wt%). For the activity control of the Pt-catalyst, the inhibitor DVS was employed. The necessary amount of the inhibitor for this MAE composition was 0.033 wt%. The crosslinker, the catalyst, and the inhibitor were also provided by Evonik Hanse GmbH.

A petri dish (diameter of 33 mm, Greiner Bio-One GmbH, Germany) was used as a mold, the bottom of which was covered with a PVC foil with a thickness of 0.1 mm. The viscous (not cured) MAE mixture was poured over the foil. The air bubbles in the MAE specimens were removed using a vacuum desiccator for ≈5 min. Finally, the MAE coated PVC foils were cured in a universal oven (Memmert UF30, Memmert GmbH, Schwabach, Germany) with air circulation, first at 80 °C for 1 h followed by 24 h at 60 °C.

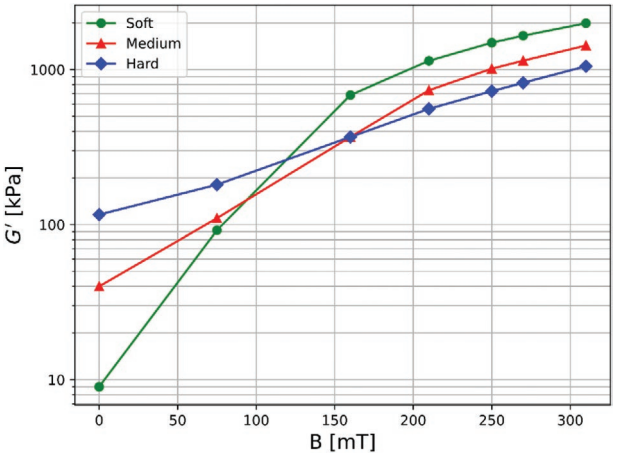

Figure 5. Magnetorheological effect $G'(B)$ [kPa] for three different MAE materials: "soft" (green circles), "medium" (red triangles), and "hard" (blue diamonds). The initial magnetization, when the magnetic field is increased from zero to the maximum value, is presented.

To characterize the MAE materials using rheological measurements, a fully cured MAE sample (without PVC foil) in the form of disk-shaped plate with a diameter of 20 mm was cut from a mold. The thickness of the MAE sample for rheological characterization corresponded to the thickness of the MAE coating. Magnetorheological measurements were performed using a commercially available rheometer (Anton Paar, model Physica MCR 301). The angular oscillation frequency ω was kept constant at 10 rad s^{-1}. This was a conventional characterization frequency for the magnetorheological effect. To avoid slippage, the normal force of ≈1 N was applied. The moduli were measured at constant strain amplitude $\gamma = 0.01\%$, which corresponded to the linear viscoelastic regime. The measurement time was 20 s per data point. The results are shown in **Figure 5**. By increasing magnetic flux density B, the storage moduli G' [kPa] of all three MAE materials strongly increased. This phenomenon is known as a magnetorheological effect.

Experimental Setup: Characterization of drop splashing was based on monitoring the splashing events with high-speed camera and backlight illumination system shown in **Figure 6**a. The samples were positioned on the top side of a custom 3D printed plastic holder, while a cylindrical neodymium iron boron magnet (grade N40, dimensions Ø25 × 10 mm)

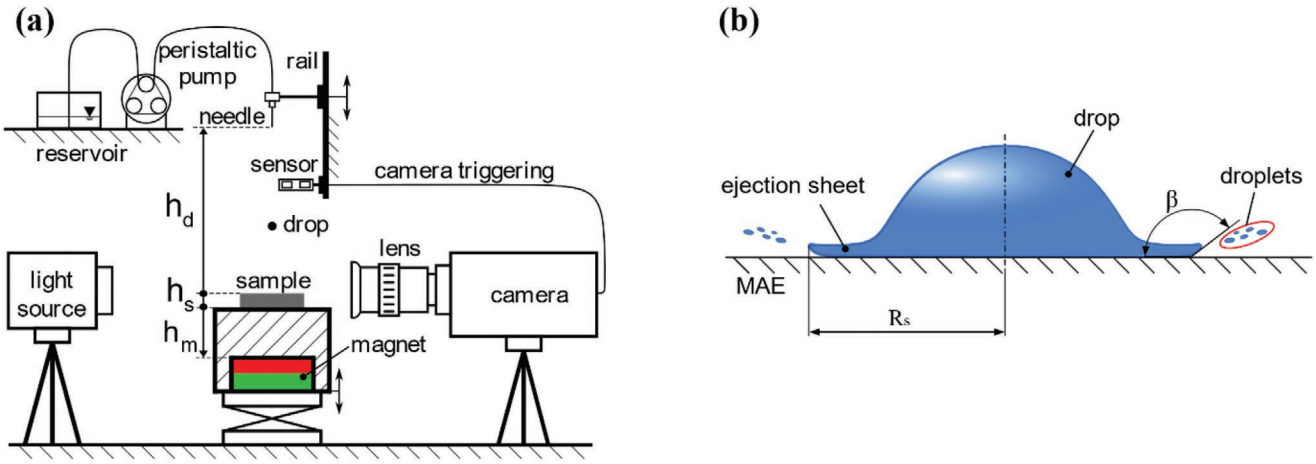

Figure 6. a) Experimental system for characterization of drop splashing on MAE samples. Relative positions of the sample, the magnet, and the injection needle used for drop release are characterized by h_s, h_m, and h_d. b) Schematic drawing of the drop shape shortly after its impact on the MAE surface.

was positioned on the bottom side. The holder construction enabled adjustment of the distance between the magnet and the sample (h_m) which resulted in a change of magnetic flux density at the sample surface. The drops hit the surface in the region near the symmetry axis of the magnet, where the magnetic field was rather homogeneous and directed perpendicular to the surface.

Ethanol (100%, Merck Emsure ACS, ISO, Reag. Ph Eur) was selected as a testing liquid, to facilitate the comparison with the experimental results reported by Howland et al.[11] Drop generation was achieved by using a peristaltic pump (Ismatec REGLO Digital, 2 channel ISM596) connected to a reservoir of ethanol on one side and a 23 gauge needle with a straight tip on the other side. The needle was mounted onto a vertical translation stage that enabled adjusting the needle height from the sample's surface h_d. This consequently defined the drop impact velocity.

Ethanol was diamagnetic. However, the magnetic susceptibility of ethanol was small: $\chi \approx 7.3 \times 10^{-6}$. Therefore, it can be considered as a non-magnetic substance. The authors were not able to detect the effect of magnetic field on ethanol drop splashing using a non-magnetic (aluminum) substrate.

The splashing events were captured using a shadowgraph video-imaging system consisting of a high-speed camera (Photron Fastcam SA-Z, model 2100K-M-64GB, resolution 1024 × 1024 pix, frame rate at a full resolution 20 000 fps) with a macro lens (Sigma model APO MACRO 180 mm F2.8 DG HSM) and a high intensity LED light projector (XHP 50 000, XLED Technology, Netherlands) with a luminous flux of 50 000 lm. A laser triangulation proximity sensor (Keyence LV-NH37, Japan) was used for triggering the camera at the moment of drop passage through its laser beam. The images were captured at 40 000 fps with a shutter time of 2.5 µs and sensor resolution of 1024 × 512 pix. The corresponding object resolution was 0.0255 mm pix^{-1} and the viewing range of 26 mm × 13 mm in a horizontal and vertical direction, respectively.

The captured images were analyzed first in the proprietary Photron software (PFV4). Then, they were further processed using custom-written Python programs to resolve the drop speed (v) and its radius (R) just before the impact. In purpose to resolve if either a splash or a deposition occurred, the splashing events of several consecutive experiments performed at the same value of h_d were analyzed. The impact sequences were examined frame by frame to detect the possible droplets breaking out from the ejection sheet. When the number of droplets in the viewing area was more than five, the outcome probability p was defined as a definite splash ($p(splash) = 1$). In contrast, the total absence of droplets was defined as a definite deposition ($p(splash) = 0$). When the number of droplets in the viewing area was between 1 and 5, the splash probability was set as $p(splash) = 0.5$.

The authors were also interested in the initial deceleration of the ejection sheet shortly after the drop impact. Its value was measured by determining the radius of the rim of the ejection sheet R_S (see Figure 6b) as a function of time and subsequently deducing its second-order time derivative at the time point $t = 25$ µs. Besides this, a dynamic contact angle β of the ejection sheet was determined as the tangent to the curve fitted to its tip with respect to the MAE surface. The aim of this analysis was to characterize surface wettability properties as a function of the magnetic field. The contact angle measurements were performed at We = 130 ± 7 and in all cases corresponded to the deposition regime, with the purpose of achieving better measuring resolution.

All experiments were performed at normal laboratory conditions at 22 ± 0.5 °C. For each set of selected parameters (type of MAE sample, magnet position h_m, the height of drop release h_d) the experiment was repeated five times. The corresponding results were given as the average values ± standard deviation.

Supporting Information

Supporting Information is available from the Wiley Online Library or from the author.

Acknowledgements

Financial support of reciprocal visits by the Slovenian Research Agency (ARRS, project no. BI-DE/20-21-11) and the German Academic Exchange Service (project no. 57513473) in the framework of the project "Smart magneto-sensitive coatings for controllable droplet splashing" is gratefully acknowledged. The authors also acknowledge financial support by the ARRS in the framework of the research programs P1-0192-Light and Matter and P2-0392-Optodynamics. I.A.B. thanks The State Conference of Women and Equality Officers at Bavarian Universities (LaKoF Bavaria) for a Ph.D. scholarship. The work of M.S. was funded by the Deutsche Forschungsgemeinschaft (DFG, German Research Foundation)—Project No. 437391117. The authors thank Gašper Glavan for useful discussions and Raphael Kriegl for preliminary investigations of the after-effect of ethanol on MAE surfaces and Tobias Probst for assistance with experiments.

Open access funding enabled and organized by Projekt DEAL.

Conflict of Interest

The authors declare no conflict of interest.

Data Availability Statement

The data that support the findings of this study are openly available in Mendeley at https://doi.org/10.17632/sv338gn9s7.1.

Keywords

drop deposition, drop splashing, dynamic contact angle, ejection sheet, magnetoactive elastomers, magneto-responsive surfaces

Received: February 15, 2021
Revised: March 12, 2021
Published online: May 5, 2021

[1] A. L. Yarin, *Annu. Rev. Fluid Mech.* **2006**, *38*, 159.
[2] T. Liu, Y. Xu, in *Smart and Functional Soft Materials* (Ed: X. Dong), IntechOpen, London **2019**.
[3] B. Derby, *Annu. Rev. Mater. Res.* **2010**, *40*, 395.
[4] G. Prashar, H. Vasudev, L. Thakur, *Eng. Failure Anal.* **2020**, *115*, 104622.
[5] H. Zhang, Y. Ma, G. Hu, Q. Liu, *Nucl. Eng. Des.* **2020**, *366*, 110757.
[6] S. Chaudhuri, S. Basu, P. Kabi, V. R. Unni, A. Saha, *Phys. Fluids* **2020**, *32*, 063309.
[7] A. L. N. Moreira, A. S. Moita, M. R. Panão, *Prog. Energy Combust. Sci.* **2010**, *36*, 554.
[8] C. Tang, M. Qin, X. Weng, X. Zhang, P. Zhang, J. Li, Z. Huang, *Int. J. Multiphase Flow* **2017**, *96*, 56.
[9] Z. Yan, R. Zhao, F. Duan, T. N. Wong, K. C. Toh, K. F. Choo, P. K. Chan, Y. S. Chua, *Two Phase Flow, Phase Change Numerical Modeling* (Ed: A. Ahsan), IntechOpen, London **2011**.
[10] G. Grant, J. Brenton, D. Drysdale, *Prog. Energy Combust. Sci.* **2000**, *26*, 79.
[11] C. J. Howland, A. Antkowiak, J. R. Castrejón-Pita, S. D. Howison, J. M. Oliver, R. W. Style, A. A. Castrejón-Pita, *Phys. Rev. Lett.* **2016**, *117*, 184502.
[12] G. Filipcsei, I. Csetneki, A. Szilágyi, M. Zrínyi, In *Oligomers – Polymer Composites – Molecular Imprinting* (Eds: B. Gong, A. R. Sanford, J. S. Ferguson), Springer, Berlin **2007**, pp. 137–189.
[13] Y. Li, J. Li, W. Li, H. Du, *Smart Mater. Struct.* **2014**, *23*, 123001.

[14] A. M. Menzel, *Phys. Rep.* **2015**, *554*, 1.
[15] Ubaidillah, J. Sutrisno, A. Purwanto, S. A. Mazlan, *Adv. Eng. Mater.* **2015**, *17*, 563.
[16] S. Odenbach, *Arch. Appl. Mech.* **2016**, *86*, 269.
[17] M. López-López, J. Durán, L. Iskakova, A. Zubarev, *J. Nanofluids* **2016**, *5*, 479.
[18] M. A. Cantera, M. Behrooz, R. F. Gibson, F. Gordaninejad, *Smart Mater. Struct.* **2017**, *26*, 023001.
[19] R. Weeber, M. Hermes, A. M. Schmidt, C. Holm, *J. Phys.: Condens. Matter* **2018**, *30*, 063002.
[20] M. Shamonin, E. Y. Kramarenko, In *Novel Magnetic Nanostructures*, 1st ed.(Eds: N. Domracheva, M. Caporali, E. Rentschler), Elsevier, Amsterdam **2018**, pp. 221–245.
[21] M. S. Saveleva, K. Eftekhari, A. Abalymov, T. E. L. Douglas, D. Volodkin, B. V. Parakhonskiy, A. G. Skirtach, *Front. Chem.* **2019**, *7*, 179.
[22] J. D. Carlson, M. R. Jolly, *Mechatronics* **2000**, *10*, 555.
[23] S. Lee, C. Yim, W. Kim, S. Jeon, *ACS Appl. Mater. Interfaces* **2015**, *7*, 19853.
[24] C. Yang, L. Wu, G. Li, *ACS Appl. Mater. Interfaces* **2018**, *10*, 20150.
[25] V. V. Sorokin, B. O. Sokolov, G. V. Stepanov, E. Y. Kramarenko, *J. Magn. Magn. Mater.* **2018**, *459*, 268.
[26] G. Glavan, P. Salamon, I. A. Belyaeva, M. Shamonin, I. Drevenšek-Olenik, *J. Appl. Polym. Sci.* **2018**, *135*, 46221.
[27] M. Watanabe, Y. Tanaka, D. Murakami, M. Tanaka, M. Kawai, T. Mitsumata, *Chem. Lett.* **2020**, *49*, 280.
[28] G. Glavan, W. Kettl, A. Brunhuber, M. Shamonin, I. Drevenšek-Olenik, *Polymers* **2019**, *11*, 594.
[29] P. A. Sánchez, E. S. Minina, S. S. Kantorovich, E. Y. Kramarenko, *Soft Matter* **2019**, *15*, 175.
[30] C. Shiwei, D. Shuai, W. Xiaojie, L. Weihua, *Smart Mater. Struct.* **2019**, *28*, 045016.
[31] R. Li, X. Li, P. Yang, J. Liu, S. Chen, *Smart Mater. Struct.* **2019**, *28*, 085018.
[32] T. A. Nadzharyan, O. V. Stolbov, Y. L. Raikher, E. Y. Kramarenko, *Soft Matter* **2019**, *15*, 9507.
[33] Y. Zhou, S. Huang, X. Tian, *Adv. Funct. Mater.* **2020**, *30*, 1906507.
[34] R. Li, D. Wang, P. Yang, X. Tang, J. Liu, X. Li, *Ind. Eng. Chem. Res.* **2020**, *59*, 9143.
[35] C. Lian, K.-H. Lee, C.-H. Lee, *Tribol. Int.* **2016**, *98*, 292.
[36] R. Li, D. Ren, X. Wang, X. Chen, S. Chen, X. Wu, *J. Intell. Mater. Syst. Struct.* **2017**, *29*, 160.
[37] R. Li, X. Li, Y. Li, P. Yang, J. Liu, *Friction* **2020**, *8*, 917.
[38] A. Ahmed, B. A. Fleck, P. R. Waghmare, *Phys. Fluids* **2018**, *30*, 077102.
[39] J. Zhou, D. Jing, *Phys. Rev. Fluids* **2019**, *4*, 083602.
[40] G. Kumar, S. Shyam, P. K. Mondal, in *Recent Advances in Mechanical Engineering* (Eds: K. M. Pandey, R. D. Misra, P. K. Patowari, U. S. Dixit), Springer, Singapore **2021**, pp. 961–968.
[41] B. Rapp, *Microfluidics: Modelling, Mechanics and Mathematics*, Elsevier, Amsterdam **2017**.
[42] S. Chougale, D. Romeis, M. Saphiannikova, *J. Magn. Magn. Mater.* **2021**, *523*, 167597.
[43] M. A. Quetzeri-Santiago, K. Yokoi, A. A. Castrejón-Pita, J. R. Castrejón-Pita, *Phys. Rev. Lett.* **2019**, *122*, 228001.
[44] L. Chen, E. Bonaccurso, M. E. R. Shanahan, *Langmuir* **2013**, *29*, 1893.
[45] L. Chen, E. Bonaccurso, P. Deng, H. Zhang, *Phys. Rev. E: Stat., Nonlinear, Soft Matter Phys.* **2016**, *94*, 063117.
[46] P. Mazurek, S. Vudayagiri, A. L. Skov, *Chem. Soc. Rev.* **2019**, *48*, 1448.
[47] J. N. Lee, C. Park, G. M. Whitesides, *Anal. Chem.* **2003**, *75*, 6544.
[48] C. Yu, C. Yu, L. Cui, Z. Song, X. Zhao, Y. Ma, L. Jiang, *Adv. Mater. Interfaces* **2017**, *4*, 1600862.
[49] J. S. Vrentas, C. M. Vrentas, *J. Appl. Polym. Sci.* **1991**, *42*, 1931.
[50] S.-H. Kim, S. Lee, D. Ahn, J. Y. Park, *Sens. Actuators, B* **2019**, *293*, 115.
[51] V. V. Sorokin, I. A. Belyaeva, M. Shamonin, E. Y. Kramarenko, *Phys. Rev. E: Stat., Nonlinear, Soft Matter Phys.* **2017**, *95*, 062501.
[52] I. A. Belyaeva, E. Y. Kramarenko, M. Shamonin, *Polymer* **2017**, *127*, 119.
[53] D. V. Saveliev, I. A. Belyaeva, D. V. Chashin, L. Y. Fetisov, D. Romeis, W. Kettl, E. Y. Kramarenko, M. Saphiannikova, G. V. Stepanov, M. Shamonin, *Materials* **2020**, *13*, 3297.